Heliyon 5 (2019) e02905

Contents lists available at ScienceDirect

Heliyon

journal homepage: www.heliyon.com

Research article

Plasmodium falciparum DDX31 is DNA helicase localized in nucleolus

Rahena Yasmin, Manish Chauhan, Suman Sourabh, Renu Tuteja *

Parasite Biology Group, ICGEB, P. O. 10504, Aruna Asaf Ali Marg, New Delhi, 110067, India

ARTICLE INFO

Keywords:
Cell biology
Bioinformatics
Microbiology
Proteins
Biochemistry
Molecular biology
ATPase
DEAD-box
Helicase
Malaria
Nucleolus
Unwinding

ABSTRACT

Malaria is a major infectious disease and is responsible for millions of infections every year. As drug resistance strains of *Plasmodium* species are emerging, there is an urgent need to understand the parasite biology and identify new drug targets. Helicases are very important enzymes that participate in various nucleic acid metabolic processes. Previously we have reported several putative DEAD box helicases in the genome of *Plasmodium falciparum* 3D7 strain. In this study, we present biochemical characterization of one of the members of Has1 (Helicase associated with SET1) family of DEAD box proteins from *P. falciparum* 3D7 strain. PfDDX31 is a homologue of human DDX31 helicase and contains all the conserved characteristics motifs. The core PfDDX31C exhibits DNA and RNA dependent ATPase activity and unwinds partially duplex DNA by utilizing ATP or dATP only. The immunofluorescence assay results show that PfDDX31 is expressed throughout all the intraerythrocytic developmental stages in *P. falciparum* 3D7 strain. The co-localization with nucleolar marker PfNop1 further suggests that PfDDX31 is mostly present in nucleolus, a discrete nuclear compartment.

1. Introduction

Malaria is one of the major mosquito-borne parasitic illnesses in many tropical and sub-tropical regions. The World Health Organization estimated that in 2018 malaria caused 219 million clinical episodes (WHO, 2018). Although five species of *Plasmodium* such as *P. vivax*, *P. falciparum*, *P. malariae*, *P. ovale* and *P. knowlesi* are main malaria causing parasites, *P. falciparum* is responsible for severe form of malaria in human (Cowman et al., 2016; Tuteja, 2007). Due to the emergence of drug resistant parasites the old therapeutic drugs became ineffective (Blasco et al., 2017). To combat this problem artemisinin-based combination therapies (ACTs) are given with one or two long-acting drugs like amodiaquine, mefloquine, sulphadoxine/pyrimethamine or lumefantrine (Nosten and White, 2007). However, the loss of efficacy of the ACTs has resulted in emergence of multiple drug resistant parasites (Dondorp et al., 2017; WHO artemisinin report, 2018). Therefore, it is important to understand the basic biology of *P. falciparum* and identify new parasite-specific chemotherapeutic targets and develop new anti-malarial drugs (Aguiar et al., 2012; Rout and Mahapatra, 2019).

Helicases play pivotal role in nucleic acid metabolism and they unwind DNA duplex or secondary structures of RNA by harnessing energy derived from ATP hydrolysis (Tuteja and Tuteja, 2004; Soultanas et al., 2000). They are classified into six super families (SF1– SF6) on the basis of the conserved motifs (Gorbalenya and Koonin, 1993). The DEAD-box proteins belong to SF2 helicases and are involved in various aspects of RNA metabolism, including nuclear transcription, ribosomal biogenesis and nucleocytoplasmic transport in human and yeast (Bates et al., 2005; Cordin et al., 2006; Daugeron and Linder, 1998). Due to the presence of amino acid sequence DEAD (Aspartic Acid-Glutamic Acid--Alanine-Aspartic Acid) in conserved motif II; these proteins are designated as DEAD box proteins. The Has1 proteins are important members of DEAD-box family (Rocak et al., 2005). In yeast Has1 proteins are characterized as the ATP-dependent RNA helicases involved in the biogenesis of 40S and 60S ribosome subunits (Dembowski et al., 2013; Rocak et al., 2005). The genome wide analysis revealed that four members of Has1 family are present in *P. falciparum* (Tuteja, 2010). Previously we have biochemically characterized PfH69 (*Plasmodium falciparum* helicase 69 kDa; PF3D7_0630900, homologue of Has1p from *P. falciparum*) and reported the essentiality of N-terminal region for its enzymatic activities (Prakash and Tuteja, 2010).

PF3D7_0721300 is a homologue of Dbp7p (DEAD box protein 7p) in yeast and DDX31 in humans (Tuteja, 2010). In this study we report the biochemical characterization of DDX31 from *P. falciparum* 3D7 strain. The PfDDX31 gene is 2700 base pairs long and encodes a protein of ~100 kDa. The core region of PfDDX31 designated as PfDDX31C is from 170 to 789 amino acids (620 amino acids) and contains all the characteristic

* Corresponding author.
E-mail addresses: renu@icgeb.res.in, renututeja@gmail.com (R. Tuteja).

https://doi.org/10.1016/j.heliyon.2019.e02905
Received 13 June 2019; Received in revised form 24 September 2019; Accepted 19 November 2019

motifs. PfDDX31C has both ssDNA and RNA dependent ATPase activity. PfDDX31C also exhibits the DNA helicase activity but no RNA helicase activity was detectable in PfDDX31C. The site-directed mutagenesis (SDM) was used to generate mutant of PfDDX31C (PfDDX31CM), where the conserved lysine was substituted with glutamic acid (K223E) in motif I (GSGKT). The PfDDX31CM showed decreased ATPase activity and no helicase activity. PfDDX31 is expressed throughout all intraerythrocytic developmental stages of *P. falciparum* 3D7 strain. The co-localization study with nucleolus marker PfNop1 (nucleolar protein 1) protein demonstrates that PfDDX31 is present in a distinct nuclear compartment, the nucleolus.

2. Methods and materials

2.1. In silico analysis

PlasmoDB database (https://www.plasmodb.org) was used to retrieve the amino acid sequences. The schematic diagrams were created using Prosite (https://prosite.expasy.org). The amino acid sequence was used for alignment with human and yeast homologue by using Clustal omega (http://www.ebi.ac.uk/Tools/msa/clustalo/). To check the evolutionary relationship among DDX31 helicases, a phylogenetic tree was constructed using the DDX31 protein sequences from various organisms with the help of online available software Phylogeny (www.phylogeny.fr) (Dereeper et al., 2008).

2.2. Parasite culture

P. falciparum 3D7 strain culture was grown in RPMI media (Invitrogen), 5 g/L Albumax I (Gibco, Thermofisher Scientific, MA, USA), 50 mg/L hypoxanthine (Sigma Aldrich, MO, USA), and 2 g/L sodium bicarbonate (Sigma Aldrich, MO, USA) and was supplemented with O+ human erythrocytes (Trager and Jensen, 1976). The synchronization of parasite culture was done using 5% sorbitol (Lambros and Vanderberg, 1979).

2.3. Cloning of PfDDX31C gene and expression and purification of recombinant proteins

Total genomic DNA was extracted from *P. falciparum* and was used as a template. Considering the presence of all the motifs, the primers were designed to amplify the core region containing catalytic domains (from 508 to 2367 bases that codes for 620 amino acids long protein). The encoded core protein (PfDDX31C, ~73 kDa) has all the characteristics motifs. The forward primer, PfDDX31CF1 (BamH1 site at 5′end) and the reverse primer, PfDDX31CR1 (with Xho1 site at 3′end) (primer 1 and 2 of Supplementary Table 1) were used for the amplification of PfDDX31C (1860 base pair) gene. The amplified product was ligated in pJET1.2 cloning vector. The transformation of the cloning vector was done using DH5α *E. coli* cells. The insert DNA was sub-cloned into expression vector pET28a+. The clone for PfDDX31C was sequenced (Macrogen, Seoul, Korea) for confirmation and the sequence was submitted to the NCBI database and the GenBank accession number is MH780884.

For generation of substitution mutation, Stratagene lightening change SDM kit from Agilent technologies (Santa Clara, CA, USA) was used according to the manufacturer's protocol. The template for SDM reaction was PfDDX31C-pET28a + clone and the primers 3 and 4 listed in Supplementary Table 1 were used. The sequence of the mutant, PfDDX31CM was submitted to the NCBI database and the GenBank accession number is MK579334.

2.4. Expression and purification of recombinant proteins and polyclonal antibody generation

To express protein, PfDDX31C-pET28a + clone was transformed into *E. coli* strain BL21 codon plus cells. The primary inoculum was incubated overnight and 2% of primary inoculum was used to inoculate secondary culture and the culture was allowed to grow till 0.8 OD. The protein expression was induced by adding 1 mM IPTG to the secondary culture and the culture was further allowed to grow at 16 °C for 12 h. Using lysis buffer of pH 7.5 (50 mM Tris–HCl, 100 mM NaCl, 0.05% Tween 20, 0.1% Triton X 100 and the protease inhibitor cocktail (Sigma Aldrich, MO, USA), the bacterial pellet was lysed and the lysate was centrifuged. After centrifugation the supernatant was collected and mixed with Ni-NTA resin (Qiagen, Hilden, Germany) equilibrated in binding buffer (50 mM Tris–HCl pH 7.5, 100 mM NaCl, 10 mM imidazole) and protease inhibitor cocktail and kept for binding for 1 h at 4 °C. Using column, Ni-NTA bound protein was passed and the column was washed with ~200 ml wash buffer (50 mM Tris–HCl pH 7.5, 100 mM NaCl and 10–50 mM imidazole) to remove non-specifically bound proteins. Using chilled elution buffer (50 mM Tris–HCl pH 7.5, 100 mM NaCl, 10% (v/v) glycerol and protease inhibitor cocktail), the recombinant His-tagged protein was eluted with different concentration of imidazole (100 mM–1 M). For checking the purity of PfDDX31C, SDS-PAGE and Western blot analysis were performed. For developing Western blot anti His-tagged antibodies conjugated with horse radish peroxidase (Sigma Aldrich, MO, USA) were used for detection.

The animals required to raise antibody were obtained from ICGEB after approval by the ICGEB Institutional Animal Ethics Committee (IAEC number- ICGEB/AH/2017/DEC/PB-3). ICGEB has the license of using animals under the registration number 18/1999/CPCSEA (dated 10/1/99). The purified PfDDX31C protein was used for raising polyclonal antibodies in mice and rabbit.

2.5. ATPase assay

The ATPase activity of PfDDX31C was assayed by measuring the released Pi from γ-^{32}P ATP. The purified PfDDX31C was mixed with buffer (20 mM Tris–HCl, pH 8.0, 8 mM DTT, 1.0 mM $MgCl_2$, 20 mM KCl, and 16 μg/ml BSA) and a mixture of (γ-^{32}P) ATP (~17 nM) and 1 mM cold (non-radioactive) ATP and the reaction was incubated for 1 h at 37 °C. ssDNA-dependent and RNA-dependent ATPase activity was monitored by adding 50 ng of M13mp19 ssDNA or 50 ng of RNA (RNA from *P. falciparum* trophozoite stage), respectively in the above reaction. After incubation the reaction mixtures were quenched on ice. 1 μl of reaction mixture was spotted onto thin layer chromatography (TLC) plate (Millipore, Darmstadt, Germany). TLC was used to separate the hydrolyzed Pi using TLC buffer (0.5 M LiCl and 1 M formic acid). The dried TLC plate was exposed to the phosphor screen and scanned using phosphoimager. Similar procedure was used to check ATPase activity of PfDDX31CM. The quantitation was done using ImageJ software (Schneider et al., 2012) (http://rsbweb.nih.gov/ij/).

To perform colorimetric ATPase assay, standard phosphate solution was prepared according to product manual protocol (BIOMOL green, Enzo life sciences, Farmingdale, NY, USA). The ATPase activity of PfDDX31C was assayed by measuring the released Pi from ATP. The purified PfDDX31C was mixed with buffer (20 mM Tris–HCl, pH 8.0, 8 mM DTT, 1 mM $MgCl_2$, 20 mM KCl, and 16 μg/ml BSA) and ATP. The reaction was incubated for 1 h at 37 °C. ssDNA-dependent and RNA-dependent ATPase activity was monitored by adding 50 ng of M13mp19 ssDNA or 50 ng of RNA (RNA from *P. falciparum* trophozoite stage), respectively. The ATPase activity assay was also performed in the absence of any nucleic acids. The absorbance of colored phosphate complex was measured at 620 nm wavelength to determine the release of inorganic phosphate.

2.6. Preparation of helicase substrates and helicase assays

The partially duplex DNA substrate was prepared using 47 mer oligodeoxynucleotide (oligonucleotide number 1 of Supplementary Table 2) and the method described previously (Ahmad and Tuteja, 2013).

For RNA helicase substrate, 13 mer and 39 mer RNA oligoribonucleotides (oligonucleotide number 2 and 3 of Supplementary Table 2) were synthesized from Sigma Aldrich and the substrate was prepared using the protocol described previously (Chauhan and Tuteja, 2019). To perform the DNA helicase assay, the reaction mixture (10 µl) contained purified protein, helicase buffer (20 mM Tris–HCl (pH 8.0), 8 mM DTT, 1 mM $MgCl_2$, 1 mM ATP, 10 mM KCl, 4% (w/v) sucrose, 80 µg/ml BSA) and ^{32}P-labelled DNA substrate. The reaction mixture was incubated for 45 min at 37 °C and the reaction was stopped by adding the helicase dye (0.3% SDS, 10 mM EDTA, 10% ficoll and 0.03% bromophenol blue). The total reaction mixtures were loaded on a 12% TBE gel. The unwound ssDNA was separated by electrophoresis. Images were taken with phosphor imager. Finally, the quantitation was done by using ImageJ software (Schneider et al., 2012). For RNA helicase assay, the same procedure was followed with 20 min incubation time and ^{32}P labeled partially duplex RNA substrate.

2.7. Immunofluorescence assay

To study the localization of PfDDX31 protein in the parasite, smears of parasite infected red blood cells of different developmental stages of *P. falciparum* 3D7 strain were prepared and fixed in chilled methanol for 20 min at −80 °C. The slides were incubated in 4 % bovine serum albumin in phosphate buffered saline (PBS) in cold room for overnight. The slides were washed two times with PBS and were incubated with anti-PfDDX31C antibody raised in rabbit at 1:200 dilutions in PBS for 2 h at room temperature. For co-localization studies of PfDDX31 with PfNop1 protein, the slides were incubated with polyclonal antibodies of PfDDX31C (raised in rabbit) at 1:200 dilutions and polyclonal antibodies of PfNop1 of 1:100 dilutions (raised in rat) at the same time. After incubation with primary antibodies, slides were washed three times with PBS-Tween and two times with PBS for 5 min each and then incubated for 1 h at 37 °C with Alexa Flour 488-conjugated (green) anti-rabbit antibody (secondary antibody) diluted 1:500 in PBS. For co-localization studies the secondary anti rabbit antibody for PfDDX31 (Alexa 488), and secondary anti rat antibody for PfNop1 (Alexa 594 (red)) were used. After incubating with antibodies, the slides were vigorously washed thrice with PBS-Tween (PBS, 0.5 % Tween 20) for 5 min each and twice with PBS for 5 min and then mounted with 4,6-diamidino-2- phenylindole (DAPI) mix antifade reagent (Life Technologies, CA, USA). Then prepared slides were viewed under a fluorescence microscope and microscopic images were collected using a Bio-Rad 2100 laser-scanning microscope attached to a Nikon TE 2000U microscope. Finally, the figures were prepared using NIS-elements package.

2.8. Western blot analysis

Mixed cultures of *P. falciparum* 3D7 parasite (including ring, trophozoite and schizont stages of parasite) were harvested from cultures with 10% parasitemia and 4% hematocrit. The lysis of infected RBCs was carried out in RPMI with 0.15% saponin for 20 min on ice followed by PBS wash. Harvesting of parasite pellets were performed by centrifugation at 3214 × g for 20 min at 4 °C. Then the parasite pellets were suspended in lysis buffer (Pierce, WI, USA) containing protease inhibitor cocktail (Roche, Basel, Switzerland) and lysed completely using freeze thaw cycles and centrifuged at 15871 × g for 30 min. The supernatants were used for SDS-PAGE analysis and the proteins were transferred using standard procedure (Eslami and Lujan, 2010). After blocking in 4% BSA for 2 h, the blots were incubated in pre-immune serum or anti-PfDDX31C antibodies (raised in rabbit, dilution 1:50) followed by detection with HRP-conjugated secondary antibodies (Bethyl laboratories, TX, USA) and incubated at room temperature for 2 h. The blots were developed by DAB (Diaminobenzidine) peroxide staining (Bio Basic Inc, Toronto, Canada).

2.9. Preparation of cDNA from total RNA and real-time PCR (qRT-PCR)

Synchronized infected RBCs were washed with PBS and total RNA was isolated from the lysate prepared from three stages (ring, trophozoite and schizont) of *P. falciparum* 3D7 strain. By using a cDNA synthesis kit (Superscript first-strand synthesis system from Invitrogen, Carlsbad, CA, USA), cDNA was prepared from total RNA. Quantitative real-time PCR was done in a Multicolor real-time PCR detection System ABI one step plus thermal cycler. The primer pair of PfDDX31RF1and PfDDX31RR1 (Primer number 5 and 6 in Supplementary Table 1) were used to detect PfDDX31 expression and 18S rRNA specific primer pair 18SF1 and 18SR1 (Primer number 7 and 8 in Supplementary Table 1) were used to detect 18S rRNA expression. Here 18S rRNA was used as endogenous reference. The reactions were performed in 10 µl volume using pure gene SYBR Green PCR master mix and 400 nM primers, according to manufacturer's instructions. The transcript level of PfDDX31 was assessed by comparing with endogenous 18S rRNA gene expression.

3. Results

3.1. In-silico analysis of PfDDX31

PF3D7_0721300 is homologue of DDX31 in human and Dbp7p in yeast. The gene is 2700 base pairs and encodes for 899 amino acids protein of ~100 kDa and its core (PfDDX31C) is from 170 to 789 (620 amino acids). PfDDX31 is slightly larger in size in comparison to its human and yeast counterpart (Supplementary Fig. 1A) and the core region contains all the nine conserved motifs (Supplementary Fig. 1B). The conservation of various amino acids in all motifs in DDX31 among *P. falciparum*, human and yeast was analyzed, and the amino acids are significantly conserved with little variation (Fig. 1A). The comparison of full length protein PfDDX31 shows 40.76% identity with the human and 37% identity with the yeast counterpart. *Plasmodium* species contain considerable sequence similarity for all motifs except single amino acid variation in motif V (Supplementary Fig. 2A). The domain analysis revealed that two major functional domains; the ATPase (ranging from 204 - 433 amino acids) and helicase (ranging from 593 -782 amino acids) are present in PfDDX31 (Fig. 1B i-ii). *Plasmodium* homologues are evolutionary related to human and yeast. The phylogenetic analysis of the amino acid sequence of PfDDX31 with the other DDX31 homologue of various organisms was performed and the results show that PfDDX31 is closer to yeast DDX31 homologue (Dbp7p) along with other *Plasmodium* species (Supplementary Fig. 2B).

3.2. Cloning, expression and purification of recombinant PfDDX31C and PfDDX31CM

We were unable to amplify the 2700 base pairs long PfDDX31 gene on repeated trials. So, the catalytic core region PfDDX31C containing all the functional domains of 1860 base pair was amplified and was subsequently cloned into pJET1.2 and pET28a + vectors. PfDDX31CM was constructed using site-directed mutagenesis kit. The lysine (K) of motif I of ATPase domain at position 223 (Fig. 1B iii) was replaced with glutamic acid (E) (Fig. 1B iv). PfDDX31C was expressed at 16 °C and purified using Ni-NTA chromatography and was subjected to SDS PAGE (Fig. 1C, lane 1) and Western blot analysis using the monoclonal anti-His antibody (Fig. 1D, lane 1). Various stages of protein purification have been shown in Supplementary Fig. 3A and 3B. PfDDX31CM (K223E) was also purified using method similar to PfDDX31C and was subjected to SDS PAGE and Western blot analysis (Fig. 1C, lane 2 and Fig. 1D, lane 2). Subsequently the purified PfDDX31C and PfDDX31CM were used for enzymatic assays. The purified PfDDX31C was also used for raising polyclonal antibodies in mice and rabbit.

3.3. ATPase assay of PfDDX31C and PfDDX31CM

Using colorimetric ATPase assay it has been shown that the ATPase activity of PfDDX31C is significantly stimulated in the presence of DNA and RNA. Whereas it shows only basal ATPase activity in the absence of any nucleic acid (Supplementary Fig. 4).

The percentage of released Pi from (γ-^{32}P) ATP was determined using different concentrations of PfDDX31C (10–150 nM) (Fig. 2A, lanes 1–6). ATPase activity of PfDDX31C increased in a concentration dependent manner. The ssDNA-dependent ATP hydrolysis was maximum (~45 %) at 150 nM (Fig. 2A, lane 6 and Fig. 2C). Whereas PfDDX31CM at 150 nM showed only ~25% ATP hydrolysis (Fig. 2B, lane 6 and Fig. 2C). Similarly, in case of RNA-dependent assay, PfDDX31 C at 150 nM hydrolyzed ~50% of ATP (Fig. 2D, lane 6 and Fig. 2F) and PfDDX31CM hydrolyzed ~25% of ATP at same concentration (Fig. 2E, lane 6 and Fig. 2F). To perform time dependent ATPase assay, 50 nM of PfDDX31C or PfDDX31CM proteins were used at various time intervals (0–60 min). PfDDX31C showed time dependent ATPase activity with ~35% hydrolysis within 60 min in the presence of DNA (Fig. 2G, lanes 1–5, and Fig. 2I) or RNA (Fig. 2J, lanes 1–5 and Fig. 2L) as co-factor. PfDDX31CM also exhibited time dependent ATPase activity but it was very low as compared to PfDDX31 C at same protein concentration in presence of DNA (Fig. 2H, lanes 1–5 and Fig. 2I) or RNA (Fig. 2K, lanes 1–5 and Fig. 2L). These observations suggest that PfDDX31C protein is an active ATPase and shows concentration and time dependent activity whereas PfDDX31CM showed reduced ATPase activity.

3.4. DNA helicase activity assay

The purified PfDDX31C or PfDDX31CM protein was used at various concentrations (2 nM–12 nM) for DNA helicase assay (Fig. 3A). PfDDX31C at 2 nM concentration unwinds ~5% of DNA substrate and maximum unwinding of ~50% was attained at 12 nM (Fig. 3A, lanes 1–4 and Fig. 3B). Whereas, PfDDX31CM did not exhibit significant DNA

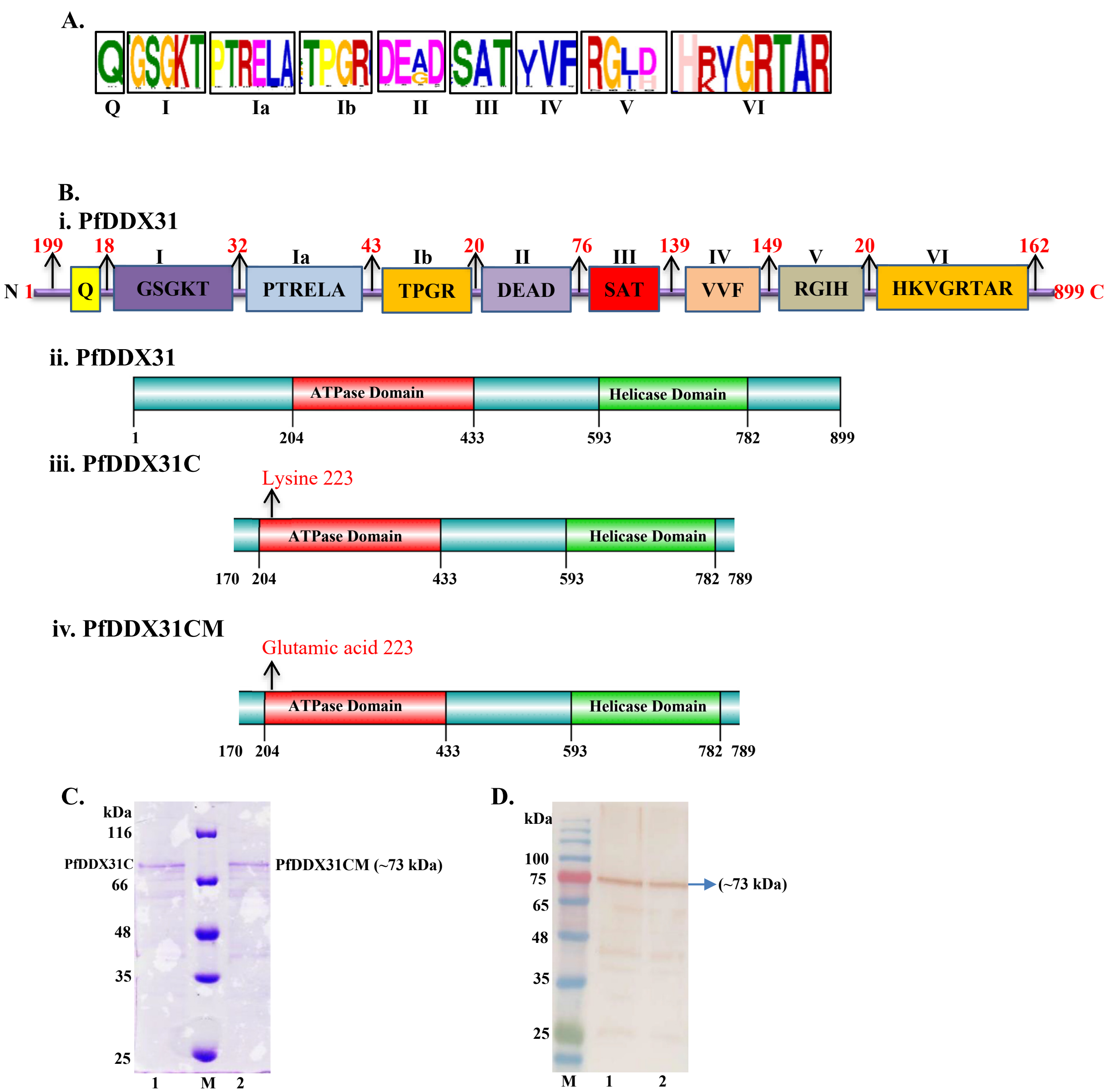

Fig. 1. Domain organization and Protein Purification. **A.** Illustration of conserved sequences of characteristic nine helicase motifs of PfDDX31 with human and yeast homologues by MEME suite; **B.** (**i**) Signature motifs of PfDDX31, Domain organization (**ii**) PfDDX31, (**iii**) PfDDX31C and (**iv**) PfDDX31CM; In (**ii-iv**) the amino acid position is also mentioned to denote the start and end of the catalytic core; **C.** Coomassie blue stained gel, lane 1, PfDDX31C and lane 2, PfDDX31CM; **D.** Western blot analysis. Lane numbers are similar to panel **C**. In panels **C** and **D**, lane M is the protein molecular weight marker.

unwinding (Fig. 3A, lanes 5–8). To assess the time dependent helicase activity 4 nM of PfDDX31 C at different time intervals was used. PfDDX31C showed time dependent DNA helicase activity and it can unwind partial duplex DNA within 15 min of the reaction with ~10% unwinding that reaches maximum of ~30% in 60 min (Fig. 3C, lanes 1–8 and Fig. 3D). PfDDX31C is an active helicase which shows concentration and time dependent helicase activity, whereas PfDDX31CM did not show helicase activity.

3.5. ATP concentration-dependent DNA helicase activity assay

To determine the optimum concentration of ATP required for

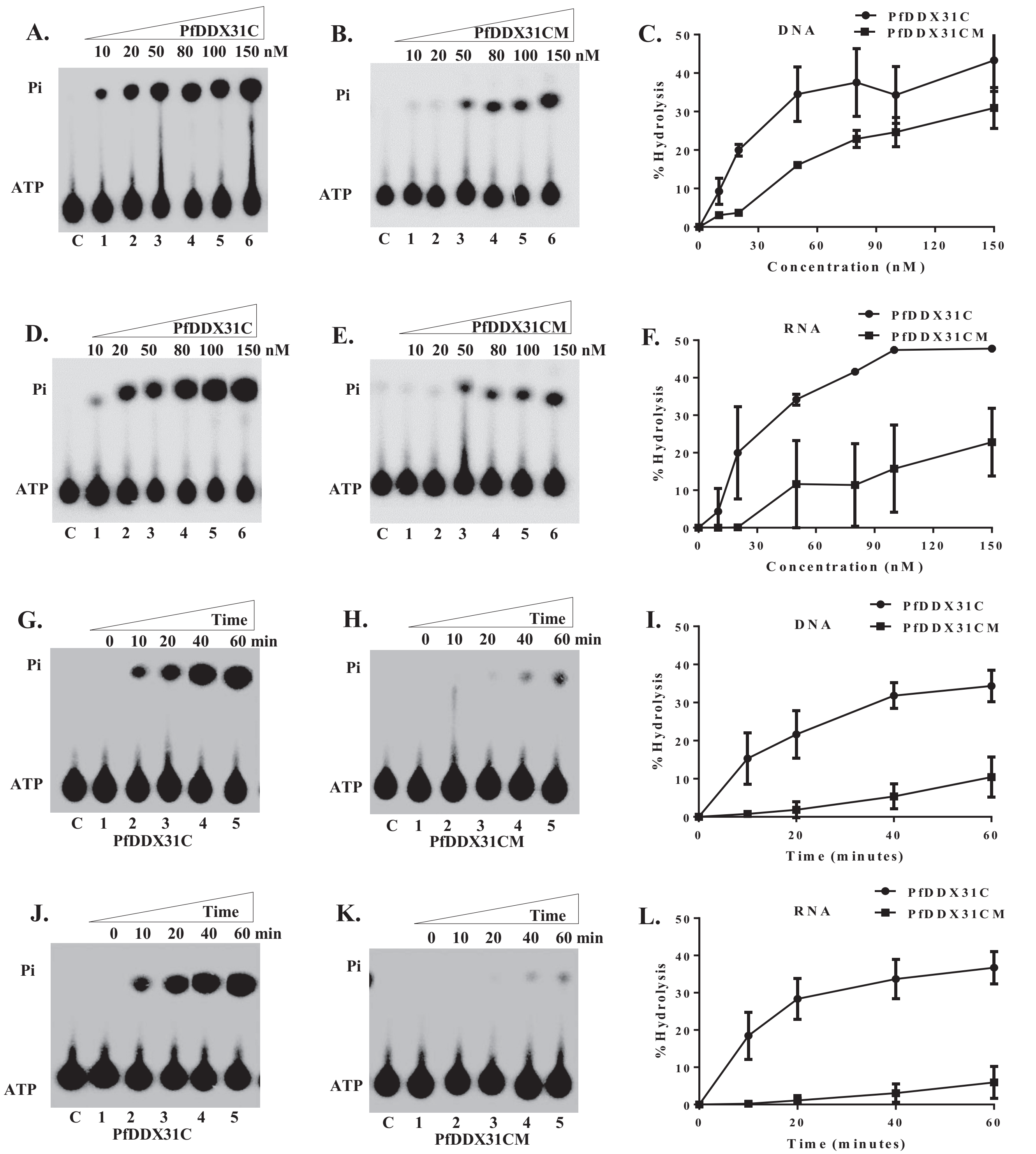

Fig. 2. ATPase activity assay. **A.** and **B.** ATPase activity with increasing concentration (10 nM–150 nM) of PfDDX31C or PfDDX31CM in the presence of DNA; **C.** Graphical representation of data of **A** and **B**, respectively; **D.** and **E.** ATPase activity with increasing concentration (10 nM–150 nM) of PfDDX31C or PfDDX31CM in the presence of RNA; **F.** Graphical representation of data of **D** and **E**, respectively; **G.** and **H.** Time dependent ATPase activity with fixed concentration (50 nM) of PfDDX31C or PfDDX31CM; in the presence of DNA; **I.** Graphical representation of data of **G** and **H** respectively; **J.** and **K.** Time-dependent ATPase activity with fixed concentration (50 nM) of PfDDX31C or PfDDX31CM; in presence of RNA; **L.** Graphical representation of data of **J** and **K**, respectively; In Panels **A**, **B**, **D**, **E**, **G**, **H**, **J**, and **K**, lane C represents control reaction without protein.

unwinding of partially duplex substrate various concentrations of ATP (0.25 mM to 5mM) were added in the reaction mixture using 4 nM of PfDDX31C (Fig. 3E, lane 2–7 and Fig. 3F). The activity was almost similar in the range of 1–3 mM ATP concentration (Fig. 3E, lanes 4–6 and Fig. 3F). But at higher ATP concentrations (5 mM), unwinding activity of PfDDX31C decreased significantly (Fig. 3E, lane 7 and Fig. 3F). In the absence of ATP, no unwinding activity of PfDDX31C was observed (Fig. 3E, lane 1).

3.6. Nucleotide dependent assay for DNA helicase activity

The helicase activity assay using 4 nM of PfDDX31C was performed in the presence of various NTPs (ATP, CTP, GTP and UTP) and dNTPs (dATP, dCTP, dGTP and dTTP). The results show that PfDDX31C exhibited significantly higher unwinding activity in the presence of ATP (27%) and dATP (25%), respectively (Fig. 3G, lanes 1–2, and Fig. 3H) and no significant unwinding was observed in the presence of other NTPs or dNTPs (Fig. 3G, lanes 3–8 and Fig. 3H).

3.7. RNA helicase activity assay

Various concentrations (2 nM–12 nM) of purified PfDDX31C or PfDDX31CM were used to perform RNA helicase assay. The results show that there is no detectable RNA helicase activity in PfDDX31C

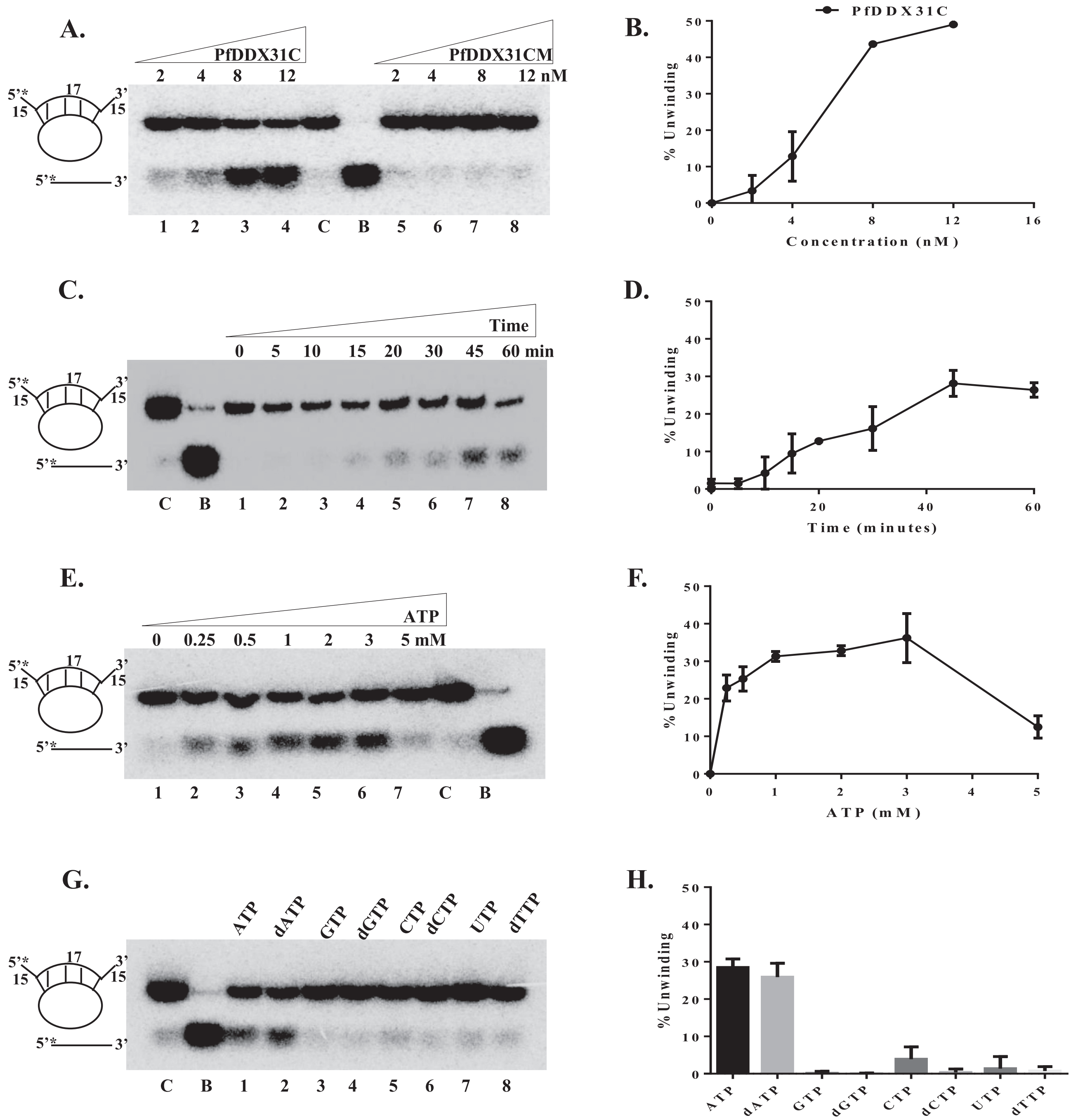

Fig. 3. Helicase activity of PfDDX31C and PfDDX31CM. **A.** Helicase activity with increasing concentration (2–12 nM) of PfDDX31C or PfDDX31CM; **B.** Quantitative analysis of data; **C.** Time dependent helicase activity with 4 nM of PfDDX31C; **D.** Quantitative analysis of data; **E.** Helicase activity with 4 nM of PfDDX31C in the presence of different concentrations of ATP; **F.** Quantitative analysis of data; **G.** Helicase activity in the presence of different types of nucleotides/deoxynucleotide triphosphates; **H.** Quantitative analysis of data; In panels **A**, **C**, **E** and **G**, lane C is the control reaction without enzyme and lane B is the boiled substrate.

(Supplementary Fig. 5, lanes 1–4) or PfDDX31CM proteins (Supplementary Fig. 5, lanes 5–8) compared to negative controls. These observations suggest that PfDDX31C only exhibits DNA helicase activity and does not show any RNA helicase activity under *in-vitro* conditions.

3.8. Localization and co-localization assay of PfDDX31 with Nop1

To study the localization of PfDDX31 protein in different developmental stages of *P. falciparum* 3D7 strain, immunofluorescence assay (IFA) was performed. The results indicate that pre-immune sera did not stain the parasite (Supplementary Fig. 6A–B, panels i–v). Staining with immune sera shows that in all stages of intraerythrocytic development of *P. falciparum* 3D7 strain, PfDDX31C is located mainly in the nucleus (Supplementary Fig. 6C–D, 6F, panels i–v) except trophozoite stage where it is mainly located in the cytosol (Supplementary Fig. 6E, panels i–v). In co-localization experiment, the anti-Nop1 antibodies were used as a nucleolar marker to confirm the localization of PfDDX31 (Figueiredo et al., 2005). It was observed that major fraction of PfDDX31 colocalized with Nop1 (Fig. 4A-E, panels i-vi) in the nucleolus. The Pearson's correlation coefficient is highest in schizont stages compared to trophozoite stage (Fig. 4A-E, panel vii). These results reveal that PfDDX31 is mainly localized in discrete nuclear region, the nucleolus. Parasite specific Western blot analysis was performed and the results demonstrate that PfDDX31C antibodies recognized a band corresponding to ~100 kDa in all intraerythrocytic developmental stages of the parasite (Fig. 4F, lanes 1–3). Here PfH45 (*P. falciparum* helicase 45) was used as a loading control. The Western blot developed using pre immune sera did not show any band (Supplementary Fig. 6G, lanes 1–3).

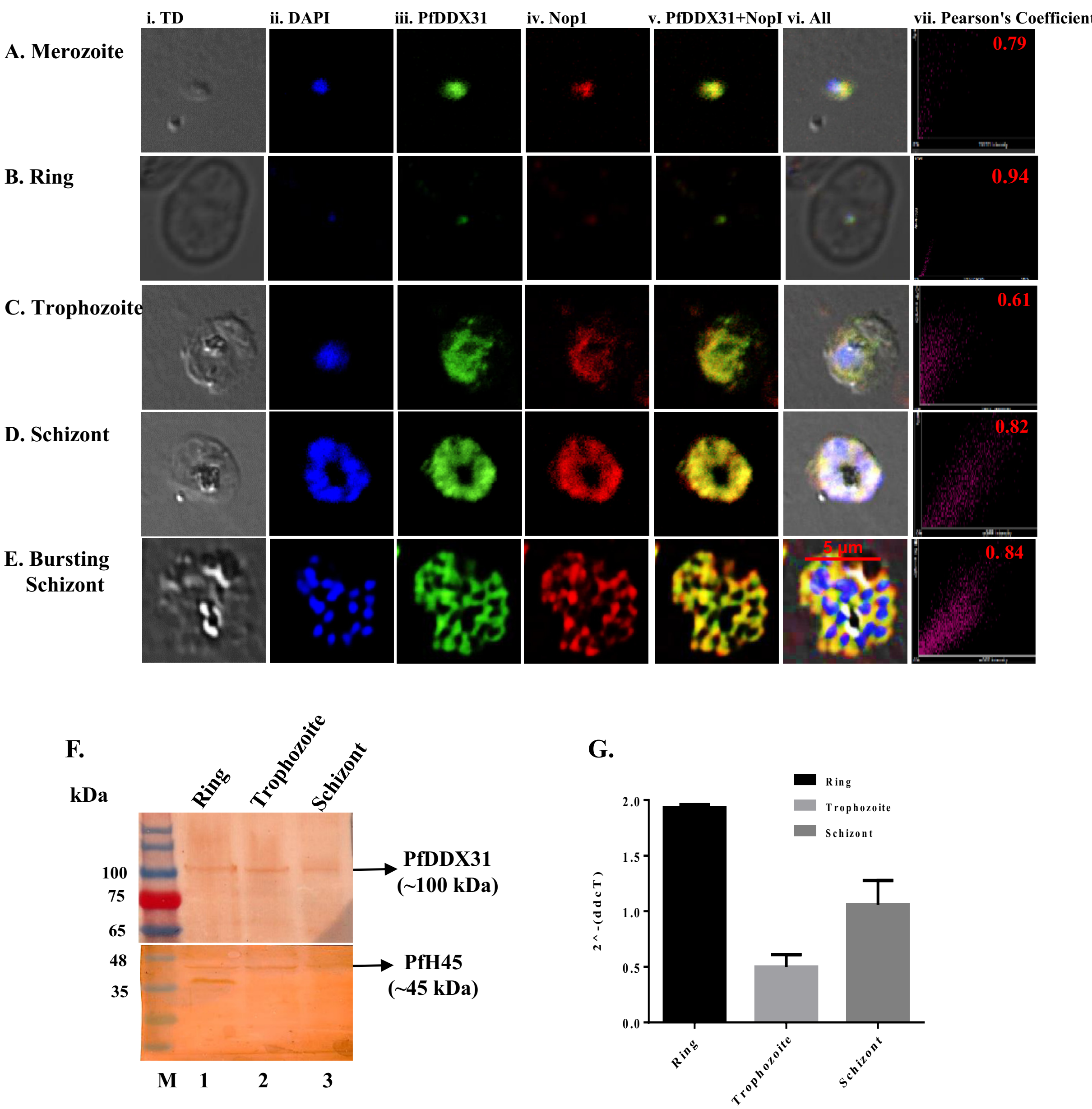

Fig. 4. Co-localization of PfDDX31 with PfNop1 protein and expression analysis through Western blot and qRT-PCR. Co-localization of PfDDX31 in intra-erythrocytic stages of *P. falciparum* 3D7 strain. In each panel, single confocal image of each stage is shown. **A-E.** stained with anti-PfDDX31 and anti-PfNop1 sera. In each panel **(i)** phase contrast (DIC) image; **(ii)** image of cell stained with DAPI (blue); **(iii)** immunofluorescent stained cell (PfDDX31); **(iv)** immunofluorescent stained cell (PfNop1); **(v)** Merged image of panel **iii** and **iv**; **(vi)** Merged image for all; **(vii)** Pearson correlation coefficient value for merged images (panel **v**); **F.** Western blot analysis of stages of *P. falciparum* 3D7; Lanes 1–3 are three different lysate preparations from ring, trophozoite and schizont stages respectively; Lane M is the pre-stained protein ladder; **G.** qRT-PCR analysis of transcript level of PfDDX31; All the values are represented as relative expression in comparison to the housekeeping 18S rRNA gene.

3.9. Gene expression analysis using qRT- PCR

The transcriptional level of PfDDX31 was investigated in asexual blood stage parasites. The total RNA was isolated, cDNA was prepared according to the method described in methods and materials section and used for the qRT-PCR assay. The expression of PfDDX31 transcript was analyzed by comparing with the expression of 18S rRNA gene. The results indicate that the expression level of PfDDX31 is highest in ring stage compared to other stages (Fig. 4G).

4. Discussion

Helicases are important for nucleic acid's metabolism such as DNA replication, repair, transcription, rRNA processing and ribosome biogenesis (Jankowsky, 2011; Putnam and Jankowsky, 2013; Tanner and Linder, 2001; Tuteja and Tuteja, 2004; Tuteja, 2017). It has been reported that *P. falciparum* contains homologues of Has1 family members of the DEAD-box family (Tuteja, 2010). This family is mainly involved in ribosomal assembly during ribosome biogenesis (Dembowski et al., 2013; Rocak et al., 2005). In this study, we have performed the bioinformatics analysis and biochemical characterization of *P. falciparum* DDX31 (PfDDX31). In-silico analysis revealed that PfDDX31 is a homologue of Dbp7p of yeast. PfDDX31C contains all the nine motifs required for ATPase and unwinding activity. The sequence of most of the motifs is highly conserved with some variation in sequence of motifs II, IV, V and VI. PfDDX31C shows both DNA and RNA dependent ATPase activity. The substitution in motif I at position 223 (GSGKT) of PfDDX31C revealed that the mutant PfDDX31CM shows decreased ATPase activity suggesting that lysine in motif I might be essential for ATP binding and hydrolysis of ATP (Rozen et al., 1989).

PfDDX31C exhibits DNA helicase activity but the mutant PfDDX31CM lacks DNA helicase activity. This loss of helicase activity might be due to loss of ATPase activity of PfDDX31CM. PfDDX31C retains its DNA helicase and ATPase activity despite lacking the N-terminus of ~20 kDa and C-terminus of ~13 kDa. It has been reported previously that the Has1 homologue PfH69 requires its N terminal along with the core region for its enzymatic activities (Prakash and Tuteja, 2010). The optimal ATP concentration range for unwinding by PfDDX31C is in between 1-3 mM PfDDX31C can unwind DNA duplex in the presence of ATP and dATP only. It was reported that PfH69 can unwind duplex DNA in the presence of all NTP/dNTPs (Prakash and Tuteja, 2010).

PfDDX31C did not exhibit any RNA helicase activity. This result is contrary to PfH69 helicase which shows dual (RNA/DNA) helicase activity (Prakash and Tuteja, 2010). The absence of RNA helicase activity might be due to the lack of N or C-terminal regions of PfDDX31C. Generally, helicases do not act alone inside the cell; they are always in association with other proteins (Jennings et al., 2008; Schütz et al., 2008). PfDDX31C might be requiring other interacting protein partners to perform duplex RNA unwinding. The co-localization studies of PfDDX31 with Nop1, a known nucleolar marker, confirmed the presence of PfDDX31 in the nucleolar region of nucleus in *P. falciparum* 3D7 strain. These results are in agreement with previous studies on DDX31 homologues (Daugeron and Linder, 1998; Fukawa et al., 2012).

The expression of PfDDX31 was observed throughout all the intraerythrocytic stages and these observations suggest that this protein might be important for the parasite growth. To the best of our knowledge this is the first report of biochemical characterization of DDX31 homologue from the malaria parasite *P. falciparum* 3D7 strain. The bi-compartmental localization of PfDDX31 mostly in the nucleolus and less in cytoplasm indicates that it is a multifunctional protein and might have different roles in different biological pathways.

Declarations

Author contribution statement

Rahena Yasmin, Manish Chauhan, Suman Sourabh: Conceived and designed the experiments; Performed the experiments; Analyzed and interpreted the data; Wrote the paper

Renu Tuteja: Conceived and designed the experiments; Analyzed and interpreted the data; Wrote the paper

Funding Statement

This work was supported by the core grant of ICGEB.

Competing interest statement

The authors declare no conflict of interest

Additional information

Data associated with this study has been deposited at GenBank under the accession numbers MH780884 and MK579334

Supplementary content related to this article has been published online at https://doi.org/10.1016/j.heliyon.2019.e02905.

Acknowledgements

The authors thank Dr. Pawan Malhotra for providing the antibodies against PfNop1.

References

Aguiar, A.C., Rocha, E.M., Souza, N.B., França, T.C., Krettli, A.U., 2012. New approaches in antimalarial drug discovery and development: a review. Memórias do Instituto Oswaldo Cruz 107, 831–845.
Ahmad, M., Tuteja, R., 2013. *Plasmodium falciparum* RuvB2 translocates in 5′–3′ direction, relocalizes during schizont stage and its enzymatic activities are up regulated by RuvB3 of the same complex. Biochim. Biophys. Acta 1834, 2795–2811.
Bates, G.J., Nicol, S.M., Wilson, B.J., 2005. The DEAD box protein p68: a novel transcriptional coactivator of the p53 tumour suppressor. EMBO J. 24, 543–553.
Blasco, B., Leroy, D., Fidock, D.A., 2017. Antimalarial drug resistance: linking *Plasmodium falciparum* parasite biology to the clinic. Nat. Med. 23, 917–928.
Chauhan, M., Tuteja, R., 2019. *Plasmodium falciparum* specific helicase 2 is a dual, bipolar helicase and is crucial for parasite growth. Sci. Rep. 9, 1–15.
Cordin, O., Banroques, J., Tanner, N.K., Linder, P., 2006. The DEAD box protein family of RNA helicases. Gene 367, 17–37.
Cowman, A.F., Healer, J., Marapana, D., Marsh, K., 2016. Malaria: biology and disease. Cell 167, 610–624.
Daugeron, M.C., Linder, P., 1998. Dbp7p, a putative ATP-dependent RNA helicase from *Saccharomyces cerevisiae*, is required for 60S ribosomal subunit assembly. RNA 4, 566–581.
Dembowski, J.A., Kuo, B., Woolford, J.L., 2013. Has1 regulates consecutive maturation and processing steps for assembly of 60S ribosomal subunits. Nucleic Acids Res. 41, 7889–7904.
Dereeper, A., Guignon, V., Blanc, G., Audic, S., Buffet, S., Chevenet, F., Dufayard, J.F., Guindon, S., Lefort, V., Lescot, M., Claverie, J.M., Gascuel, O., 2008. Phylogeny.fr: robust phylogenetic analysis for the non-specialist. Nucleic Acids Res. 36, 465–469.
Dondorp, A.M., Smithuis, F.M., Woodrow, C., Seidlein, L.V., 2017. How to contain artemisinin- and multidrug-resistant falciparum malaria. Trends Parasitol. l33, 353–363.
Eslami, A., Lujan, J., 2010. Western blotting: sample preparation to detection. J. Vis. Exp. 44, 1–2.
Figueiredo, L.M., Rocha, E.P.C., Mancio-Silva, L., Prevost, C., Hernandez-Verdun, D., Scherf, A., 2005. The unusually large *Plasmodium* telomerase reverse-transcriptase localizes in a discrete compartment associated with the nucleolus. Nucleic Acids Res. 33, 1111–1122.
Fukawa, T., Ono, M., Matsuo, T., Uehara, H., Miki, T., Nakamura, Y., Kanayama, H., Katagiri, T., 2012. DDX31 regulates the p53- HDM2 pathway and rRNA gene transcription through its interaction with NPM1 in renal cell carcinomas. Cancer Res. 72, 5867–5877.
Gorbalenya, A.E., Koonin, E.V., 1993. Helicases: amino acid sequence comparisons and structure-function relationships. Curr. Opin. Struct. Biol. 3, 419–429.
Jankowsky, E., 2011. RNA helicases at work: binding and rearranging. Trends Biochem. Sci. 36, 19–29.
Jennings, T.A., Chen, Y., Sikora, D., Harrison, M.K., Sikora, B., Huang, L., Jankowsky, E., Fairman, M.E., Cameron, C.E., Raney, K.D., 2008. RNA unwinding activity of the

hepatitis C virus NS3 helicase is modulated by the NS5B polymerase. Biochemistry 47, 1126–1135.
Lambros, C., Vanderberg, J.P., 1979. Synchronization of *Plasmodium falciparum*. J. Parasitol. 65, 418–420.
Nosten, F., White, N.J., 2007. Artemisinin-based combination treatment of falciparum malaria. Am. J. Trop. Med. Hyg. 77, 181–192.
Prakash, K., Tuteja, R., 2010. A novel DEAD box helicase Has1p from *Plasmodium falciparum*: N-terminal is essential for activity. Parasitol. Int. 59, 271–277.
Putnam, A.A., Jankowsky, E., 2013. DEAD-box helicases as integrators of RNA, nucleotide and protein binding. Biochim. Biophys. Acta 1829, 884–893.
Rocak, S., Emery, B., Tanner, N.K., Linder, P., 2005. Characterization of the ATPase and unwinding activities of the yeast DEAD-box protein Has1p and the analysis of the roles of the conserved motifs. Nucleic Acids Res. 33, 999–1009.
Rout, S., Mahapatra, R.K., 2019. *Plasmodium falciparum*: multidrug resistance. Chem. Biol. Drug Des. 1–23.
Rozen, F., Pelletier, J., Trachsel, H., Sonenberg, N., 1989. A lysine substitution in the ATP-binding site of eukaryotic initiation factor 4A abrogates nucleotide-binding activity. Mol. Cell. Biol. 9, 4061–4063.
Schneider, C.A., Rasband, W.S., Eliceiri, K.W., 2012. NIH Image to ImageJ: 25 years of image analysis. Nat. Methods. 9, 671–675.
Schütz, P., Bumann, M., Oberholzer, A.E., Bieniossek, C., Trachsel, H., Altmann, M., Baumann, U., 2008. Crystal structure of the yeast eIF4A-eIF4G complex: an RNA-helicase controlled by protein–protein interactions. Proc. Natl. Acad. Sci. 105, 9564–9569.
Soultanas, P., Dillingham, M.S., Wiley, P., Webb, M.R., Wigley, D.B., 2000. Uncoupling DNA translocation and helicase activity in PcrA: direct evidence for an active mechanism. EMBO J. 19, 3799–3810.
Tanner, N.K., Linder, P., 2001. DExD/H box RNA helicases: from generic motors to specific dissociation functions. Mol. Cell. 8, 251–262.
Trager, W., Jensen, J.B., 1976. Human malaria parasites in continuous culture. Science. 193, 673–675.
Tuteja, R., 2007. Malaria - an overview. FEBS J. 274, 4670–4679.
Tuteja, R., 2010. Genome wide identification of *Plasmodium falciparum* helicases: a comparison with human host. Cell Cycle. 9, 104–120.
Tuteja, R., 2017. Unraveling the importance of the malaria parasite helicases. FEBS J. 284, 2592–2603.
Tuteja, N., Tuteja, R., 2004. Unraveling DNA helicases. Motif, structure, mechanism and function. Eur. J. Biochem. 271, 1849–1863.
WHO, 2018. World Malaria Report 2018. https://www.who.int/malaria/publications/world-malaria-report-2018/en/.
WHO, August 2018. Status Report on Artemisinin and ACT Resistance. https://www.who.int/malaria/publications/atoz/artemisinin-resistance-august2018/en/.